Redox Biology 52 (2022) 102305

Contents lists available at ScienceDirect

Redox Biology

journal homepage: www.elsevier.com/locate/redox

XBP1 deficiency promotes hepatocyte pyroptosis by impairing mitophagy to activate mtDNA-cGAS-STING signaling in macrophages during acute liver injury

Zheng Liu [a,b,1], Mingming Wang [a,b,1], Xun Wang [a,b,1], Qingfa Bu [a,b], Qi Wang [a,c], Wantong Su [a,b], Lei Li [a,b], Haoming Zhou [a,b,**], Ling Lu [a,b,*]

[a] Hepatobiliary Center, The First Affiliated Hospital of Nanjing Medical University, Research Unit of Liver Transplantation and Transplant Immunology, Chinese Academy of Medical Sciences, Nanjing, China
[b] Jiangsu Key Laboratory of Cancer Biomarkers, Prevention and Treatment, Collaborative Innovation Center for Cancer Personalized Medicine, Nanjing Medical University, Nanjing, China
[c] School of Medicine, Southeast University, Nanjing, China

ARTICLE INFO

Keywords:
Acute liver injury
XBP1
Pyroptosis
Mitophagy
STING

ABSTRACT

Hepatocellular cell death and macrophage proinflammatory activation contribute to the pathology of various liver diseases, during which XBP1 plays an important role. However, the function and mechanism of XBP1 in thioacetamide (TAA)-induced acute liver injury (ALI) remains unknown. Here, we investigated the effects of XBP1 inhibition on promoting hepatocellular pyroptosis to activate macrophage STING signaling during ALI. While both TAA- and LPS-induced ALI triggered XBP1 activation in hepatocytes, hepatocyte-specific XBP1 knockout mice exhibited exacerbated ALI with increased hepatocellular pyroptosis and enhanced macrophage STING activation. Mechanistically, mtDNA released from TAA-stressed hepatocytes could be engulfed by macrophages, further inducing macrophage STING activation in a cGAS- and dose-dependent manner. XBP1 deficiency increased ROS production to promote hepatocellular pyroptosis by activating NLRP3/caspase-1/GSDMD signaling, which facilitated the extracellular release of mtDNA. Moreover, impaired mitophagy was found in XBP1 deficient hepatocytes, which was reversed by PINK1 overexpression. Mitophagy restoration also inhibited macrophage STING activation and ALI in XBP1 deficient mice. Activation of XBP1-mediated hepatocellular mitophagy and pyroptosis and macrophage STING signaling pathway were observed in human livers with ALI. Collectively, these findings demonstrate that XBP1 deficiency promotes hepatocyte pyroptosis by impairing mitophagy to activate mtDNA/cGAS/STING signaling of macrophages, providing potential therapeutic targets for ALI.

1. Introduction

Pyroptosis, a recently discovered form of lytic programmed cell death, is characterized by rapid plasma membrane rupture with the consequent release of intracellular contents and proinflammatory mediators. Gasdermin D (GSDMD) acts as an effector for pyroptosis by forming pores within the plasma membrane leading to water influx, lysis, and cell death [1]. Mitochondrial DNA (mtDNA) damage can activate NLRP3 inflammasome signaling and subsequently causing caspase-1-dependent pyroptosis [2].

Free radical-mediated oxidative stress is implicated in the pathogenesis of various types of liver diseases [3]. Although mitochondria are the primary organelles for reactive oxygen species (ROS) production, ROS also mediate mitochondrial damage. Mitophagy is an evolutionarily conserved cellular process that removes dysfunctional or superfluous mitochondria, playing a critical role in maintaining mitochondrial homeostasis and cell survival [4]. Mitophagy blockade increases mitochondrial damage and pyroptosis [5]. Functional

* Corresponding author. Hepatobiliary Center, The First Affiliated Hospital of Nanjing Medical University, 300 Guangzhou Road, Nanjing, 210029, China.
** Corresponding author. Hepatobiliary Center, The First Affiliated Hospital of Nanjing Medical University, Research Unit of Liver Transplantation and Transplant Immunology, Chinese Academy of Medical Sciences, Nanjing, China.
E-mail addresses: hmzhou@njmu.edu.cn (H. Zhou), lvling@njmu.edu.cn (L. Lu).
[1] These authors contributed equally to this work.

https://doi.org/10.1016/j.redox.2022.102305
Received 17 February 2022; Received in revised form 13 March 2022; Accepted 25 March 2022
Available online 28 March 2022

interplays between endoplasmic reticulum (ER) stress, mitophagy and ROS have been revealed [3]. Mitochondria is the main source of ROS. Mitophagy, a mechanism to removed and recycled dysfunctional mitochondria [6], plays a critical role in mitochondrial ROS scavenge [7]. ROS induces the unfolded protein response (UPR) and XBP1 splicing, leading to autophagy activation [8].

XBP1 is a pivotal component of the ER stress response. XBP1 mRNA spliced by the inositol-requiring enzyme 1a (IRE1a) produces the active transcription factor sXBP1. In response to ER stress, cells initiate the unfolding protein response (UPR) to maintain intracellular homeostasis and survival [9]. Studies have also reported the regulatory role of XBP1 in ER stress signaling in the immune response and inflammation [10] and ER stress-driven pyroptosis [11,12]. In a cadmium-induced nephrotoxicity model, IRE-1a/XBP-1s signaling was responsible for NLRP3 inflammasome activation and pyroptosis of renal tubular epithelial cells [13].

The liver is the primary organ that eliminates various recently used drugs and foreign pathogens, making it one of the most vulnerable targets for toxins and acute injury. Hepatocellular injury and cell death are not only hallmarks of acute liver injury (ALI), but they also activate the intrahepatic inflammatory response by releasing various damage-associated molecular patterns (DAMPs). Macrophages, one of the highest non-parenchymal cells in the liver, plays an important role in many types of acute and chronic liver diseases. The cyclic GMP–AMP synthase (cGAS)-stimulator of interferon genes (STING) pathway is a crucial signaling cascade of the innate immune system activated by cytosolic DNA. The critical role of cGAS-STING signaling has been demonstrated in a variety of liver diseases, which include viral hepatitis, non-alcoholic fatty liver disease, alcoholic liver disease, primary hepatocellular cancer, and hepatic ischemia-reperfusion injury [14]. However, little is known about the function of XBP1 in hepatocellular pyroptosis and macrophage sting activation and its regulatory role in TAA-induced ALI.

Our objective was to investigate the effects of XBP1 on hepatocellular pyroptosis and macrophage sting activation during ALI. Here, we report that XBP1 depletion in hepatocytes aggravates hepatocellular pyroptosis, facilitateing the extracellular release of mtDNA to enhance macrophage STING activation. Mechanistically, XBP1 deficiency promotes mitochondrial ROS production by impairing mitophagy, leading to enhanced NLRP3/caspase-1/GSDMD activation and pyroptosis of hepatocytes. Alteration of these pathways is implicated in human ALI and is potentially amenable to therapeutic targeting.

2. Materials and methods

2.1. Patients and specimens

Five patients with ALI and five control patients with haemangioma without ALI undergoing partial liver resection (Supplementary Table 1) in the First Affiliated Hospital of Nanjing Medical University were enrolled in the current study. Liver biopsy specimens from patients with ALI or peri-tumor normal tissues from control patients were collected. Informed consent was obtained from each patient. All procedures that involved human samples were approved by the Ethics Committee of the Affiliated Hospital of Nanjing Medical University (Institutional Review Board approval number 2020-SRFA-220).

2.2. Animals

Hepatocyte-specific Xbp1 knockout (HKO) mice were generated by breeding Xbp1-LoxP with Alb-Cre mice (Nanjing Biomedical Research Institute of Nanjing University). Briefly, homozygous $Xbp1^{loxP/loxP}$ mice were first bred with homozygous Alb-Cre mice, and the heterozygous offspring (for both Xbp1 and Cre) were back-crossed with homozygous $Xbp1^{loxP/loxP}$ mice. Mice were housed and maintained under a 12-h light/12-h dark cycle with ad libitum access to water and standard chow with supplements under specific pathogen-free conditions. All animals were treated humanely, and all animal procedures met the relevant legal and ethical requirements according to the protocols (number NMU08-092) approved by the Institutional Animal Care and Use Committee of Nanjing Medical University.

2.3. Mouse acute liver injury induced by TAA and LPS

Male $Xbp1^{loxP/loxP}$ (WT) and HKO mice (8-week-old) were intraperitoneally injected with 300 mg/kg TAA (Sigma, Saint Louis, MO, USA) or lipopolysaccharide (LPS, 5 mg/kg, Sigma, USA) dissolved in phosphate-buffered saline (PBS). The same volume of PBS was intraperitoneally injected into the control mice. Mice were sacrificed 24 h after TAA treatment or 6 h after LPS challenge. In some experiments, mice were intraperitoneally administered chloroquine (CQ, 60 mg/kg, Sigma, Saint Louis, MO, USA), MitoTEMPO (20 mg/kg, Sigma), or AC-YVAD-cmk (8 mg/kg, Sigma) 1 h before TAA or LPS injection. Mice were intraperitoneally injected with 1 mg/kg of tunicamycin (TM, Sigma) and sacrificed 6 h after injection.

2.4. Hepatocellular function assay

Blood samples were centrifuged to obtain serum, and the levels of aspartate aminotransferase (ALT) and alanine aminotransferase (AST) were measured using an automatic chemical analyzer (Olympus Company, Tokyo, Japan).

2.5. Terminal deoxynucleotidyl transferase dUTP nick-end labeling (TUNEL) assay

Sections of paraffin-embedded hepatic tissue were washed with PBS and fixed with 4% polyformaldehyde and then incubated with a TUNEL reaction mixture (Roche, Basel, Switzerland). Briefly, slides were rinsed twice with PBS. Next, 50 μ l TUNEL reaction mixture was added to samples, which were incubated for 60 min at $37^{\circ}C$ in a humidified atmosphere in the dark. Slides were rinsed three times with PBS. Samples were analyzed in a drop of PBS under a fluorescence microscope at this state, using an excitation wavelength in the range of 450–500 nm and detection in the range of 515–565 nm (green).

2.6. Histopathology and immunohistochemical staining

Liver tissue sections (4-μ m-thick) were stained using haematoxylin and eosin (H&E) to observe inflammation and tissue damage using light microscopy. F4/80 and STING were identified by immunofluorescence using a primary rat anti-mouse F4/80 (1:100, ab11101, Abcam) and STING (1:200, #13647S, Cell Signaling Technology) antibodies, and secondary biotinylated goat anti-rat IgG (1:100, BA-1000, Vector) according to the manufacturer's instructions. Positive cells were counted blindly at 10 HPE/section.

2.7. Bone marrow-derived macrophage (BMDM) culture

Bone marrow cells were isolated from the mouse femurs and tibias as previously described [15]. BMDMs were then re-plated and cultured overnight in new culture dishes for further experiments.

2.8. Isolation of liver cells

Primary hepatocytes and liver intrahepatic macrophages were isolated by a two-stage collagenase perfusion method as described previously [15]. Primary hepatocytes were stimulated with lipopolysaccharide (LPS; 1 μ g/mL, 6 h) followed by treatment with nigericin (20 μ M, 1 h) in the presence or absence of NLRP3 inhibitor MCC950 (10 μ M) and treated with TM (2 μ g/ml) for 3 h to induce ER-stress. In some experiments, cells were pre-treated with chloroquine (CQ, 10 μ M), MitoTEMPO (50 μ M), or AC-YVAD-cmk (25 μ g/mL) for 1

h prior to TAA (70 μ M, 6 h) with or without MCC950 (10 μ M) administration. BMDMs and intrahepatic macrophages were treated with or without mtDNA isolated from primary hepatocytes for 12 h, and the cells and supernatants were harvested for further analysis.

2.9. Measurement of ROS levels

Two kinds of fluorescent probes were used to detect intracellular ROS in liver tissues and cells, namely the ROS-sensitive probe 2′,7′-dichlorodihydrofluorescein diacetate (H_2DCFDA), and dihydroethidium (DHE). For DHE staining, cryosections were incubated with 10 μ M DHE at 37°*C* for 30 min. For ROS detection in cultured cells, the cells were seeded in a 96-well plate and incubated with H_2DCFDA. Fluorescence was detected by a confocal microscope system and flow cytometry at 488 nm excitation and 525 nm emission.

2.10. Measurement of malondialdehyde (MDA), superoxide dismutase (SOD) and ROS levels and the ratio of GSH/GSSG

MDA, GSH, GSSG, SOD and ROS levels were estimated using commercial kits. Liver tissues were washed with PBS, homogenized in lysis buffer and sonicated. After being sonicated, the lysed tissue was centrifuged (10,000×*g*, 10 min) to remove debris and retain the supernatant. A microplate reader was used to measure the levels of MDA, GSH, GSSG, SOD and ROS in the supernatant. In addition, MDA, GSH, GSSG, SOD, and ROS levels were normalized according to the protein concentration.

2.11. Adeno-associated virus (AAV)-mediated gene transfer

For knockdown cGAS or overexpression of PINK1, the AAV vectors carrying cGAS shRNA or control shRNA and AAV overexpressed PINK1 or AAV-enhanced green fluorescent protein (eGFP) (Shanghai GeneChem) were intravenously injected into the tail vein of 8-week-old WT or HKO male mice at a dose of $4 \times 1{,}0^{11}$ plaque-forming units per mouse.

2.12. Lentiviral knock down of cGAS in BMDMs

BMDMs were prepared and infected with control or cGAS-siRNA lentiviruses (Shanghai GeneChem) for 72 h at 37 °C in the presence of 4 mg/ml polybrene. BMDMs were then washed and cultured in fresh medium for 24 h before mtDNA stimulation for further analysis.

2.13. mtDNA isolation and quantification

DNA was extracted from 200 μ l of cells culture supernatant of untreated and treated primary murine hepatocytes using the QIAmp DNA mini kit (QIAGEN, Duesseldorf, Germany) according to the manufacturer's instructions. Real-time polymerase chain reaction (qPCR) was performed for the quantification of mtDNA. mtDNA was quantified using mouse mt-ATP6 primers/Taqman 5′ FAM-3′ MGB probe (Bio-Rad, Hercules, CA, USA). The mitochondrial lysate of primary hepatocytes was used to isolate mtDNA using a mitochondrial DNA isolation kit (Abcam) according to the manufacturer's instructions. Total DNA was isolated using the DNeasy Blood and Tissue Kit (QIAGEN) following the manufacturer's instructions. RT-qPCR analysis was performed using a sequence detection system (ABI Prism 7000, Applied Biosystems, Foster City, CA, USA/Invitrogen, Carlsbad, CA, USA) with an SYBR green 1-step kit (Invitrogen). To evaluate the possibility of BMDMs engulfing mtDNA released from hepatocytes, mtDNA isolated from primary murine hepatocytes was tagged with Cy5-dCTP (Amersham Cy5-dCTP, GE Healthcare) using PCR, as described by the manufacturer (BioPrime DNA Labeling system, Life Technologies). The Cy5-labeled DNA PCR was cleaned with a DNeasy Mini Spin Column (QIAGEN) before the DNA concentration was measured using a Nanodrop (Thermo Scientific).

2.14. Mitochondria and cytosolic dsDNA measurements

The PicoGreen dsDNA Reagent and Kit (Invitrogen, no. P11496) and MitoTracker Red CMXRos (Invitrogen, no. M5712) were used at 0.3% v/v and 100 nM in serum-free DMEM for 30 min at 37 °*C* to co-localize dsDNA and mitochondria. To determine the mitochondrial membrane potential, cells were stained with tetramethylrhodamine methyl ester (100 nM; Invitrogen, no. I34361) for 15 min. Stained cells were then examined using a confocal microscope system (LSM880, Carl Zeiss, Inc.) equipped with a 63 × 1.2 NA objective lens (Carl Zeiss, Inc.).

2.15. Immunofluorescence staining

LC3 in primary hepatocytes and F4/80 and STING in macrophages were identified using immunofluorescence with rabbit anti-mouse LC3B mAb (1:200, #83506S, Cell Signaling Technology), rat anti-mouse F4/80 mAb (1:200, ab6640, Abcam), and rabbit anti-mouse STING mAb (1:200, 19851-1-AP, Proteintech). Thereafter, they were incubated with secondary Cy3-conjugated goat anti-rabbit IgG (1:100, AP132C, Sigma) and FITC-conjugated goat anti-rat IgG (1:100, AP136F, Sigma) according to the manufacturer's instructions. 4′,6-diamidino-2-phenylindole and Hoechst 33,342 (Thermo Scientific, no. 62249) were used for nuclear staining. To assess pyroptosis, active caspase-1 was measured using the FLICA reagent FAM-YVAD-FMK (FAM-FLICA Caspase-1 Assay Kit, ImmunoChemistry Technologies, USA) according to the manufacturer's instructions, and propidium iodide (PI) was used to mark cells with membrane pores. Stained sections were imaged with a confocal microscope system LSM880 (Zeiss) and analyzed using Zen software (Zeiss).

2.16. Western blot analysis

Proteins were extracted from liver tissue or cells using ice-cold lysis buffer (50 mM Tris, 150 mM Nacl, 1% sodium deoxycholate, 0.1% sodium dodecyl sulfate and 1% Triton-100). Proteins (20 μ g/sample) were subjected to 10% sodium dodecyl sulfate-polyacrylamide gel electrophoresis and transferred to polyvinylidene difluoride nitrocellulose membranes (Bio-Rad). Anti-rabbit cGAS (1:1000, #31659S), STING (1:1000, #13647S), P-TBK1 (1:1000, #5483S), P-IRF3 (1:1000, #29047S), P–NF–κ B (1:1000, #3033S), NLRP3 (1:1000, #15101S), cleaved caspase-1 (1:1000, #89332S), P62 (1:1000, #23214S), LC3B (1:1000, #43566S) and anti-mouse β-actin (1:1000, #3700S) antibody were from Cell Signaling Technology; Anti-rabbit XBP1 (1:1000, ab37152) and GSDMD (1:1000, ab209845) antibody were from Abcam.

2.17. Quantitative real-time-PCR

Total RNA was purified from cells using TRIzol reagent (Invitrogen) according to the manufacturer's instructions. Reverse transcription into cDNA was performed using a Transcriptor First-Strand cDNA Synthesis kit (Roche). Quantitative real-time PCR was performed using SYBR green (Roche) on a StepOnePlus Real-Time PCR System (Applied Biosystems). Quantitative PCR was repeated three times. The expression levels of target genes were normalized to that of hypoxanthine phosphoribosyltransferase.

2.18. Transmission electron microscopy

Transmission electron microscopy of hepatocytes was performed according to the manufacturer's instructions. The sections were further stained with 0.3% lead citrate and imaged using an electron microscope (HITACHI, Tokyo, Japan; 4000 × or 30,000 × magnification).

2.19. Enzyme-linked immunosorbent assay (ELISA)

Cytokine/chemokine levels (IL-1β, IL-18, MCP-1, and CXCL-10) were measured using ELISA kits according to the manufacturer's protocols

(Thermo Fisher Scientific).

2.20. Statistical analyses

Data are expressed as the mean ± SEM. Two-group comparisons were performed using two-tailed student's t-tests, comparisons between multiple groups were performed using one-way or two-way ANOVA with Tukey's multiple comparisons. All statistical analyses were performed using STAT software, version 11.0.

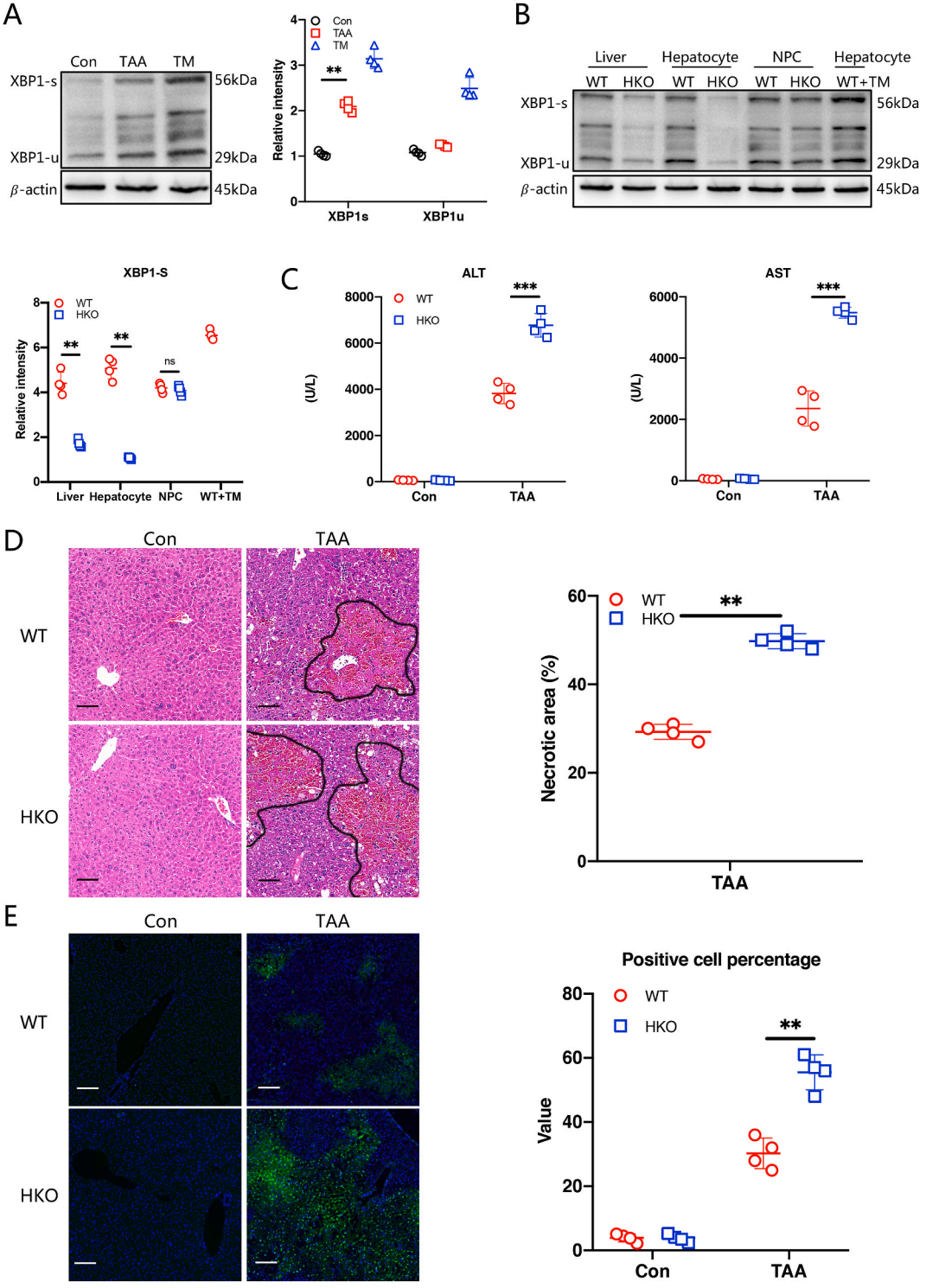

Fig. 1. Hepatocyte-specific XBP1 deficiency aggravated TAA-induced acute liver injury.
(A and B) Western blot analysis of XBP1-s, XBP1-u, and β-actin levels in liver tissues, hepatocytes, and liver non-parenchymal cells (NPCs). Full-length blots are presented in Supplementary Figs. 8A and B. (C) Serum ALT and AST levels. (D) H&E staining of the liver tissue sections. Scale bar, 50 μm. (E) TUNEL assay (green) was used to detect DNA fragmentation in the livers, and DAPI (blue) was used as a counterstain. Scale bar, 50 μm. Data are presented as the mean ± SEM (n = 4). *P < 0.05, **P < 0.01, ***P < 0.001. NS, not significant; ALT, alanine aminotransferase; AST, aspartate aminotransferase. (For interpretation of the references to colour in this figure legend, the reader is referred to the Web version of this article.)

3. Results

3.1. Hepatocyte-specific XBP1 deficiency aggravated TAA-induced ALI

We first examined XBP1 protein levels in the liver after TAA or PBS treatment. Significantly increased protein and mRNA levels of XBP1 were observed in the livers after TAA treatment (Fig. 1A and Supplementary Fig. 1A). To better understand the functions of XBP1 in regulating hepatocyte cell injury following TAA treatment, we used the Cre-LoxP system to create hepatocyte-specific XBP1 KO mice. In these HKO mice, XBP1 expression was significantly decreased in liver tissues and deficient in hepatocytes, although similar in liver non-parenchymal cells (Fig. 1B). Hepatocyte XBP1 depletion aggravated TAA-induced liver injury as evidenced by higher levels of serum ALT and AST (Fig. 1C), exacerbated architectural destruction (Fig. 1D), and increased hepatocellular cell death (Fig. 1E). The liver proinflammatory immune

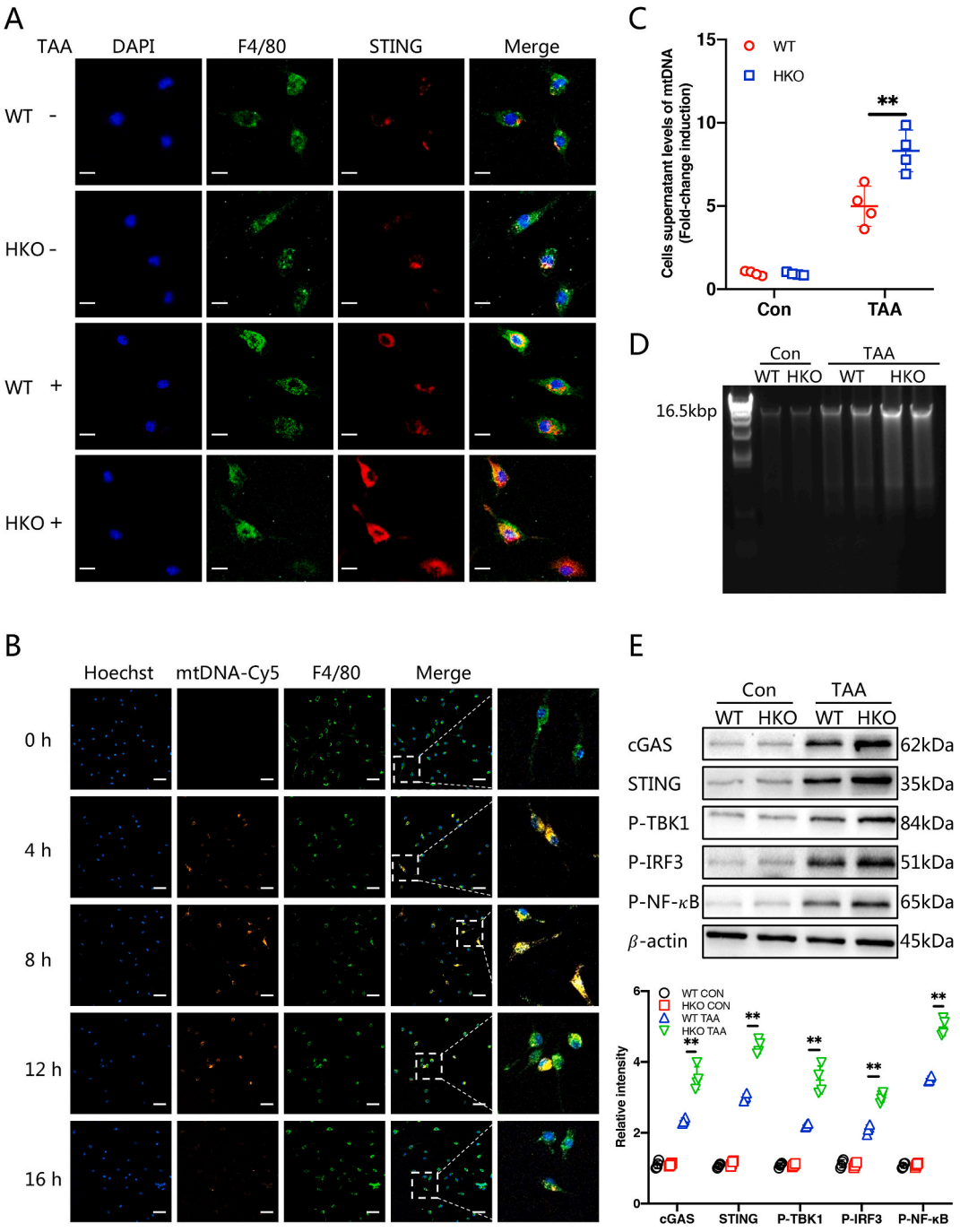

Fig. 2. XBP1 deficiency promoted mtDNA release from TAA-stressed hepatocytes to activate macrophage STING signaling.
(A) Intrahepatic macrophages were isolated from livers post TAA treatment followed by staining of STING (red), F4/80 (green), and nucleus (blue). Scale bar, 100 μm. (B) BMDMs were treated with mtDNA (tagged with Cy5-dCTP) isolated from primary hepatocytes and then stained with F4/80 (green) and Hoechst 33,342 (blue) at different time points. Scale bar, 100 μm. (C–E) Primary hepatocytes were stimulated with or without TAA for 6 h and then the supernatant was collected. mtDNA levels in the supernatant were analyzed using RT-qPCR (C) and agarose electrophoresis (D). (E) BMDMs were stimulated with the above supernatant and subjected to Western blot analysis for cGAS, STING, P-TBK1, P-IRF3, P–NF–κ B and β-actin levels. Data are presented as the mean ± SEM (n = 4). *P < 0.05, **P < 0.01, ***P < 0.001. NS, not significant. (For interpretation of the references to colour in this figure legend, the reader is referred to the Web version of this article.)

response was exacerbated in XBP1 HKO mice as shown by increased proinflammatory cytokine/chemokine gene expression induction and protein expression (Supplementary Figs. 1B and C). Much more F4/80-positive macrophages were significantly more abundant in the livers of HKO mice than that in those of WT controls after TAA treatment (Supplementary Fig. 1D). Summarily, these data suggested that XBP1 deficiency in hepatocytes aggravated TAA-induced ALI and macrophage-related intrahepatic inflammation.

3.2. XBP1 deficiency promoted mtDNA release from TAA-stressed hepatocytes to activate macrophage STING signaling

STING-mediated macrophage proinflammatory response was reported in a variety of liver diseases [14]. Thus, we hypothesized that macrophage STING signaling functions in regulating TAA-induced ALI. Intrahepatic macrophages were isolated from the livers after TAA treatment, and the STING signaling pathway was analyzed. Macrophages from HKO mice showed enhanced activation of the STING signaling pathway in macrophages, as evidenced by enhanced STING staining (Fig. 2A) and increased protein levels of cGAS, STING, P-TBK1, P-IRF3, and p–NF–kB (Supplementary Fig. 3A).

We previously found that mtDNA release from hepatocytes contributes to STING activation of macrophages [16]. Next, we investigated if enhanced macrophage STING activation was caused by increased mtDNA release from XBP1 deficient hepatocytes. To test this hypothesis, BMDMs were stimulated with isolated mtDNA or supernatant from TAA-treated primary hepatocytes. Results showed that mtDNA-Cy5 was engulfed by BMDMs early at 4 h and peaked at 12 h post-co-culture of mtDNA-Cy5 with BMDMs (Fig. 2B). Dose-dependence of mtDNA stimulation in activating cGAS-STING signaling (Supplementary Fig. 2A) and the subsequent proinflammatory response of macrophages (Supplementary Figs. 3B and C) were also observed, indicateing that increased mtDNA release from hepatocytes might contribute to enhanced macrophage STING activation, as observed in HKO mice.

Thus, we next measured the extracellular release of mtDNA from hepatocytes in WT and HKO mice after TAA treatment. Primary hepatocytes were isolated from HKO mice after TAA treatment and cultured *in vitro*, and then the supernatant levels of mtDNA were analyzed. The results showed that hepatocytes from HKO mice released increased levels of mtDNA in the supernatant (Fig. 2C and D). Stimulation of BMDMs with the above supernatant effectively activated STING signaling in macrophages. BMDMs stimulated with the supernatant of hepatocytes from HKO mice showed enhanced STING signaling (Fig. 2E).

We also evaluated the direct effect of TAA treatment on mtDNA modification, which may further modulate macrophage STING activation. BMDMs stimulated with the same dose of mtDNA isolated from primary hepatocytes with or without TAA pre-treatment showed a similar level of cGAS-STING activation (Supplementary Fig. 3B) and subsequent proinflammatory response (Supplementary Fig. 3C). Moreover, treatment of mitoTEMPO, a specific ROS scavenger of mitochondria, decreased mtDNA level in the cell supernatant of cultured primary hepatocytes post TAA treatment (Supplementary Fig. 3D), indicating an important role of mtDNA, but not other dsDNA, in the activation of STING signaling. Collectively, these results indicated that XBP1 deficiency promoted extracellular mtDNA release from TAA-stressed hepatocytes to activate macrophage STING signaling.

3.3. Hepatocyte-derived mtDNA promoted macrophage STING activation in a cGAS-dependent manner

cGAS activation induced by dsDNA functions in the synthesis of cGAMP and subsequent activation of the STING signaling pathway. To further examine the role of the mtDNA-cGAS-STING signaling axis in regulating proinflammatory macrophage response, we blocked macrophage cGAS activation by AAV-cGAS-shRNA in vivo (Supplementary Fig. 4A). Immunohistochemistry analysis of STING in liver tissues showed that inhibition of cGAS activation in macrophages decreased intrahepatic STING activation (Fig. 3A). Furthermore, blockade of cGAS activation reversed the upregulation of STING signaling pathway activation (Fig. 3B) and proinflammatory cytokine and chemokine production (Fig. 3C) of intrahepatic macrophages by hepatocyte XBP1 depletion. Functionally, in vivo blockade of cGAS activation in macrophages abrogated the role of hepatocyte XBP1 depletion in aggravating TAA-induced liver injury, as evidenced by the analysis of serum levels of ALT and AST, pathological examination, and TUNEL staining (Supplementary Figs. 4B–D). Reduced infiltration of F4/80-positive macrophage infiltration (Supplementary Fig. 4E) and decreased intrahepatic inflammation (Supplementary Fig. 4F) were also observed after cGAS inhibition.

Subsequently, we blocked cGAS activation in BMDMs after mtDNA stimulation *in vitro*. Consistent with the above in vivo findings, cGAS inhibition significantly decreased STING signaling activation in BMDMs after mtDNA activation, as evidenced by Western blot analysis and STING staining (Fig. 3D and E). Collectively, these results indicated that cGAS signalling played an essential role in regulating macrophage STING activation by mtDNA released from hepatocytes.

3.4. XBP1 deficiency facilitated mtDNA extracellular release by inducing hepatocyte pyroptosis

Pyroptosis is a lytic programmed cell death characterised by rapid plasma membrane rupture and the release of proinflammatory intracellular contents. We investigated whether hepatocyte pyroptosis could be induced by TAA and its role in promoting the extracellular release of mtDNA. Primary hepatocytes were isolated from WT and HKO mice and then treated with TAA or LPS combined with nigericin. Both TAA and LPS treatment with nigericin induced primary hepatocytes pyroptosis, which was exacerbated by XBP1 depletion. MCC950, a pyroptosis inhibitor, abrogated the role of hepatocyte XBP1 depletion in aggravating hepatocytes pyroptosis (Fig. 4A). The NLRP3/caspase-1/GSDMD signaling axis of pyroptosis in hepatocytes was also activated by TAA treatment and enhanced by XBP1 depletion (Fig. 4B). Enhanced caspase-1 staining was observed in XBP1 deficient hepatocytes (Fig. 4C). To further determine the functional importance of pyroptosis in regulating the extracellular release of mtDNA, YVAD-cmk was used to block caspase-1 activation and subsequent hepatocellular pyroptosis. As expected, blockade of caspase-1 activation effectively inhibited the cleavage of the N-terminal domain of GSDMD (Fig. 4D). Positive staining of cytosolic dsDNA was observed in the area around the mitochondria after TAA treatment, which was inhibited by the caspase-1 blockade. XBP1 depletion enhanced peri-mitochondrial dsDNA staining and was reversed by caspase-1 blockade (Fig. 4E). Semiquantitative analysis of cytosolic mtDNA established that XBP1 depletion enhanced caspase-1-mediated pyroptosis leading to increased cytosolic mtDNA accumulation (Fig. 4F). Furthermore, increased levels of mtDNA were observed in the supernatant of cultured XBP1-deficient hepatocytes after TAA treatment, which could be reversed by caspase-1 inhibition as well (Fig. 4G). Thus, these results suggested that XBP1 depletion promoted pyroptosis in hepatocytes induced by TAA treatment, facilitating mtDNA cytosolic accumulation and extracellular release.

3.5. Mitochondrial ROS production was essential for XBP1 deficiency to promote hepatocyte pyroptosis

ROS play an important role in regulating TAA-induced liver injury and GSDMD activation. We analyzed the effects of mitochondrial ROS on hepatocyte pyroptosis. Evidently, TAA treatment induced intrahepatic oxidative response as shown by analyzing MDA, GSH/GSSG, SOD, and ROS levels in liver tissues, which were enhanced by XBP1 depletion (Fig. 5A–E). Increased mitochondrial membrane permeability was observed in XPB1-deficient hepatocytes (Fig. 5F). MitoTEMPO, a

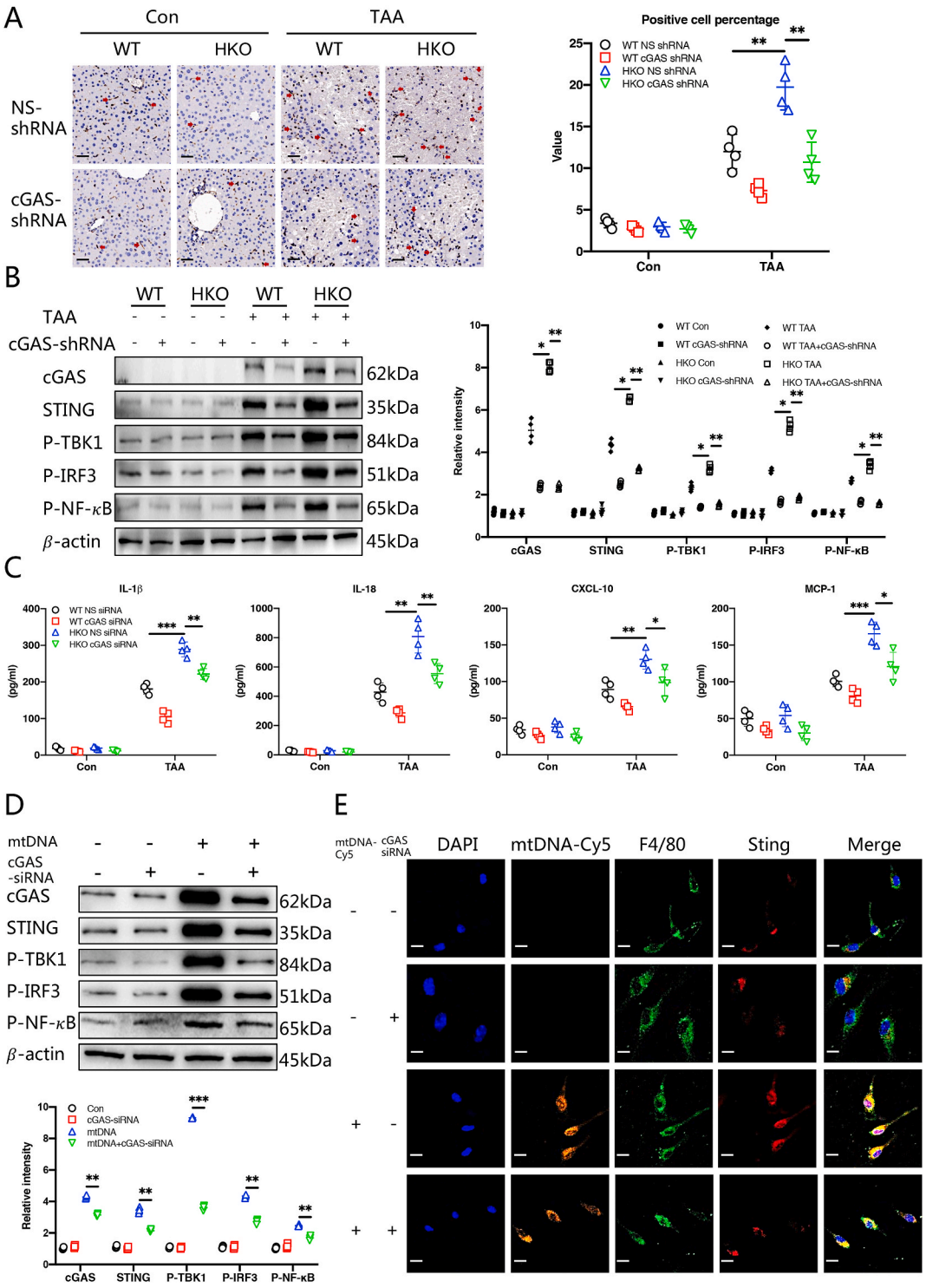

Fig. 3. Hepatocyte-derived mtDNA promoted macrophage STING activation in a cGAS-dependent manner.
(A–C) WT and HKO mice were pre-treated with AAV-cGAS-shRNA or AAV-control-shRNA 7 days before TAA administration. (A) STING staining of liver tissue sections. Scale bar, 50 μm. (B) Intrahepatic macrophages were isolated and protein levels of cGAS, STING, P-TBK1, P-IRF3, P–NF-κ*B* and β-actin were analyzed using western blotting. (C) Serum cytokine/chemokine levels (IL-1 β, IL-18, MCP-1 and CXCL-10) were measured using ELISA. (D and E) BMDMs were transfected with cGAS-siRNA or non-specific siRNA (Control) lentiviral particles and then stimulated with 100 ng/ml of mtDNA. Protein levels of cGAS, STING, P-TBK1, P-IRF3, P–NF-κ*B* and β-actin were measured using western blotting (D). (E) BMDMs were treated with Cy5-dCTP-tagged mtDNA (100 ng/ml) for 12 h and stained with F4/80 (green), STING (red), and Hoechst 33,342 (blue). Scale bar, 100 μm. Data are presented as the mean ± SEM (n = 4). *P < 0.05, **P < 0.01, ***P < 0.001. NS, not significant. (For interpretation of the references to colour in this figure legend, the reader is referred to the Web version of this article.)

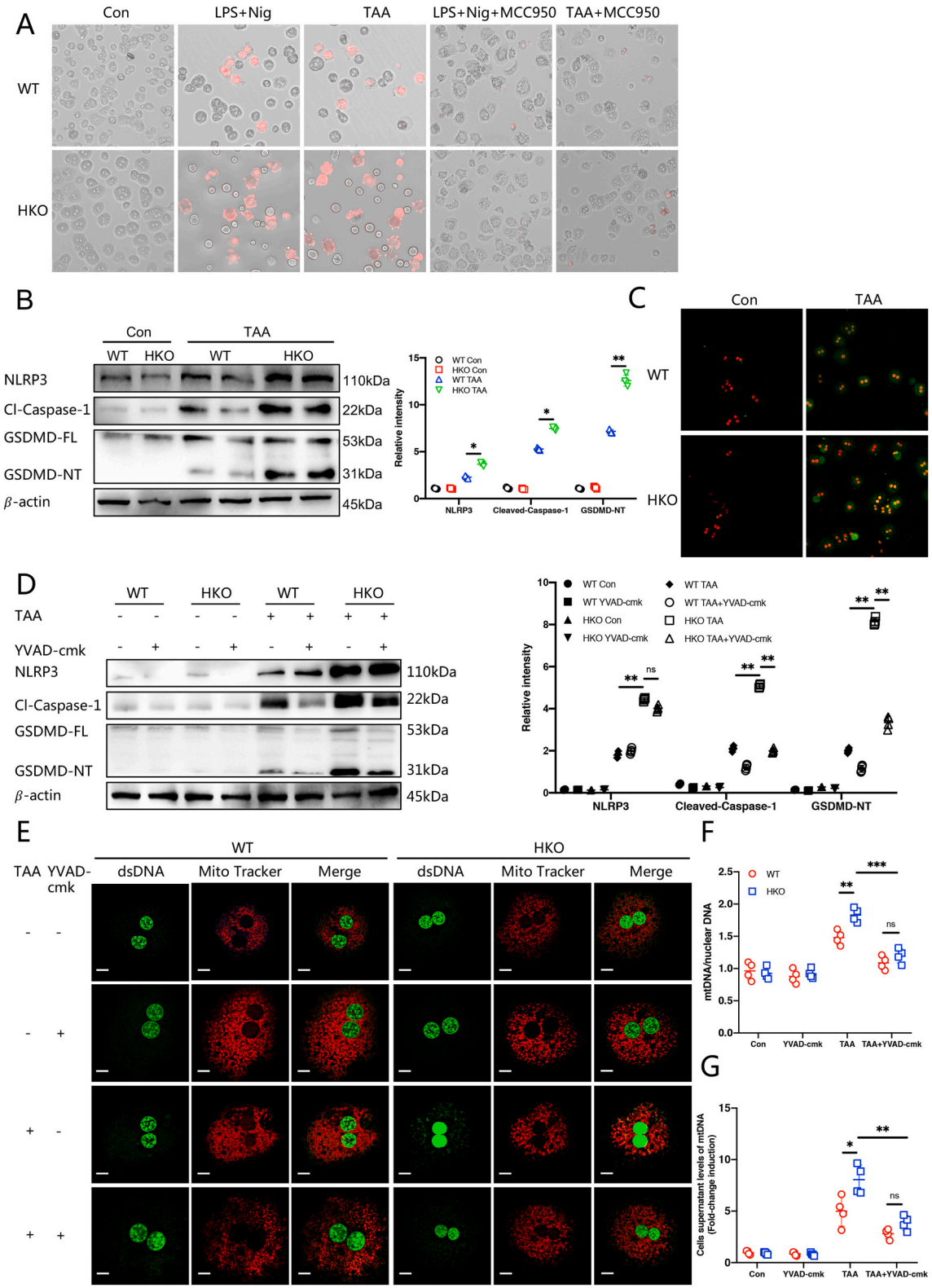

Fig. 4. XBP1 deficiency facilitated mtDNA extracellular release by inducing hepatocyte pyroptosis.
(A) WT or XBP1 deficient primary hepatocytes were treated with TAA or LPS + Nig and stained with PI. Scale bar, 100 μm. (B–G) Primary hepatocytes were stimulated with TAA with or without YVAD-cmk pre-treatment. Representative Western blot analysis of NLRP3, GSDMD-FL, GSDMD-NT, cleaved caspase-1, and β-actin (B). FLICA caspase-1 activity (green) and PI staining; scale bar = 100 μm (C). Western blot analysis of NLRP3, GSDMD-FL, GSDMD-NT, cleaved caspase-1, and β-actin levels (D). MitoTracker (red) and dsDNA (green) staining. Scale bar, 100 μm (E). Mitochondrial gene Dloop1 level normalized to nuclear gene Tert quantified using RT-qPCR in the cytoplasm of hepatocytes (F). The levels of mtDNA in the supernatant of hepatocytes were measured using RT-qPCR (G). Data are presented as the mean ± SEM (n = 4). *P < 0.05, **P < 0.01, ***P < 0.001. NS, not significant; PI, propidium iodide. (For interpretation of the references to colour in this figure legend, the reader is referred to the Web version of this article.)

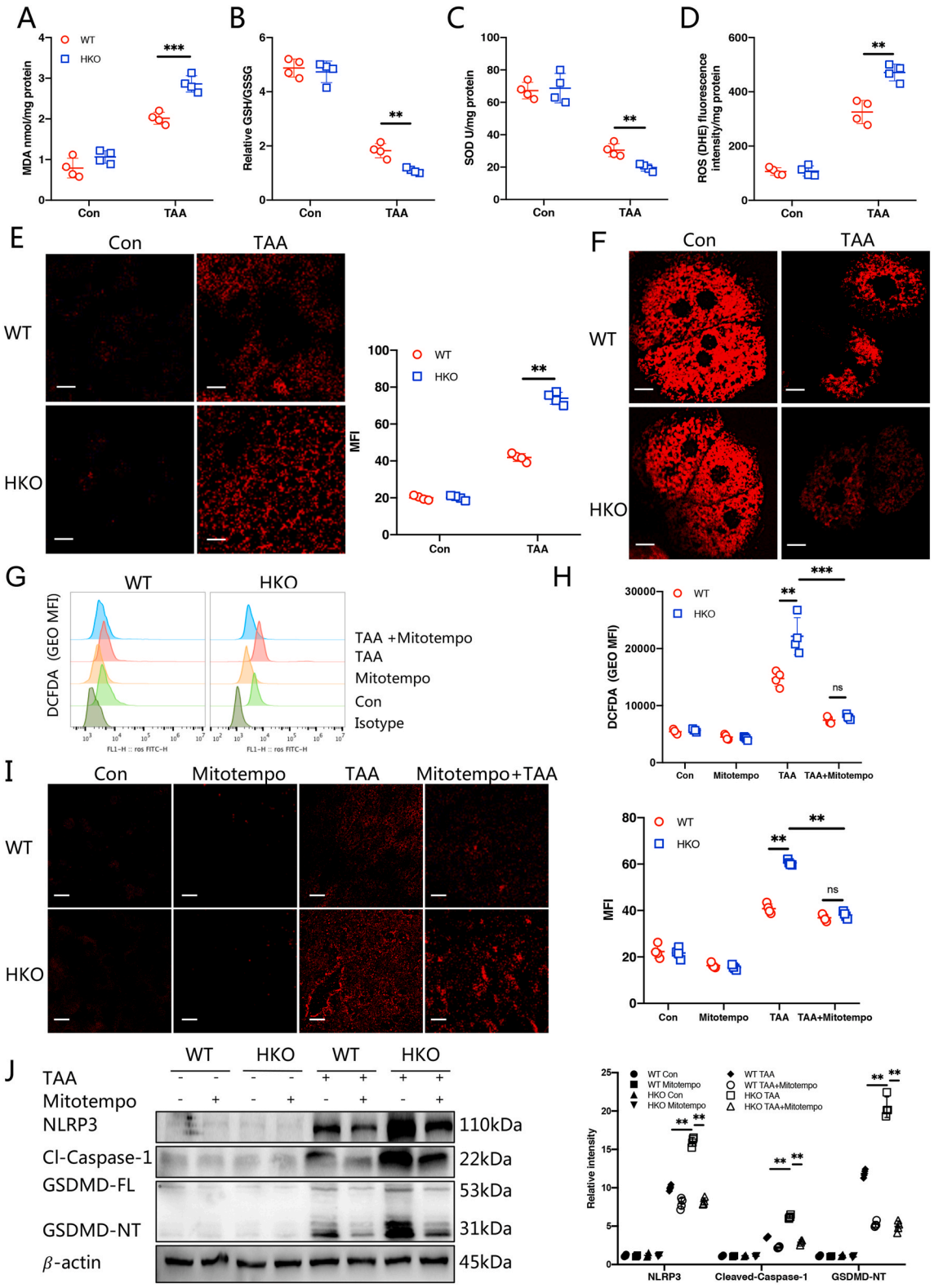

Fig. 5. Mitochondrial ROS production was essential for XBP1 deficiency to promote hepatocyte pyroptosis.
(A–E, I) Mice were administered TAA. MDA (A) and GSH/GSSG (B) levels and SOD (C) activity in the liver tissues. ROS levels in the liver tissues were determined using a tissue ROS test kit (D). Representative images of the fluorescence assay of ROS in liver tissues, quantified using the fluorescent probe DHE (red); scale bar, 50 μm (E). (F) Primary hepatocytes were treated with TAA and stained with tetramethylrhodamine methyl ester (red). Scale bar, 100 μm. (G and H) Primary hepatocytes were treated with TAA with or without MitoTEMPO pre-treatment. ROS levels were detected by DCFDA fluorescence. (I and J) Mice were subjected to TAA administration with or without MitoTEMPO pre-treatment. Representative images of the fluorescence assay of ROS in liver tissues using the fluorescent probe DHE (red). Scale bar, 50 μm (I). Representative Western blot images of NLRP3, GSDMD-FL, GSDMD-NT, cleaved caspase-1, and β-actin levels in isolated primary hepatocytes (J). Data are presented as the mean ± SEM (n = 4). *P < 0.05, **P < 0.01, ***P < 0.001. NS, not significant; DHE, dihydroethidium. (For interpretation of the references to colour in this figure legend, the reader is referred to the Web version of this article.)

specific mitochondrial ROS scavenger significantly reduced ROS expression in hepatocytes following TAA treatment (Fig. 5G–I). Furthermore, ROS scavenging by MitoTEMPO inhibited the activation of NLRP3-caspase-1-GSDMD signaling in hepatocytes and abrogated the role of XBP1 depletion in promoting pyroptosis signaling activation (Fig. 5J). These findings suggested that mitochondrial ROS played an essential role in mediating the activation of NLRP3-caspase-1-GSDMD signaling and was essential for XBP1 deficiency to promote pyroptosis in hepatocytes.

3.6. Impaired mitophagy contributed to ROS-mediated pyroptosis of XBP1 deficient hepatocytes and subsequent macrophage STING activation during TAA-induced ALI

The interplay between ER stress and mitophagy has recently been reported. Impaired mitophagy may result in the accumulation of damaged mitochondria and the dysregulation of free radical scavenging. We investigated if increased mitochondrial ROS expression was caused by impaired mitophagy in XBP1 deficient hepatocytes. TAA treatment promoted mitophagy activation, as shown by the enhanced LC3 staining in primary hepatocytes from WT mice. Contrastingly, no significant difference in LC3 staining was observed in hepatocytes from HKO mice (Fig. 6A). LC3 immunofluorescence staining of liver tissues confirmed the results (Supplementary Fig. 5A). Electron microscopy analysis demonstrated that acute TAA treatment induced the appearance of mitophagosomes, and XBP1 depletion blocked mitophagosome formation (Fig. 6B). We observed that there were higher levels of LC3-II and lower levels of p62 in hepatocytes isolated from WT mice post-TAA treatment, compared to corresponding levels in hepatocytes isolated from HKO mice. After TAA treatment, enhanced activation of mitophagy signaling by Pink1 and Parkin was observed in WT hepatocytes after TAA treatment (Fig. 6C). Autophagic flux was then analyzed, and results showed that CQ treatment caused a further increase in LC3-II, only in WT and not in XBP1-deficient hepatocytes after TAA treatment, indicating that XBP1 activation promoted autophagic flux of hepatocytes during TAA-induced injury (Fig. 6D).

To further investigate the role of mitophagy in regulating mtDNA release from hepatocytes and subsequent STING activation of macrophages, CQ was used to block mitophagy activation in vivo. Evidently, mitophagy blockade resulted in an increased oxidative response in WT hepatocytes, whereas no significant effects were found in XBP1 deficient hepatocytes (Fig. 6E–H). An increase in the extracellular release of mtDNA was observed by mitophagy inhibition in WT hepatocytes (Fig. 6I). Enhanced NLRP3-caspase-1-GSDMD activation in hepatocytes, cGAS-STING activation in macrophages, and intrahepatic inflammation were found in WT mice after CQ treatment (Fig. 6J, Supplementary Figs. 5B and C). Mitophagy inhibition also aggravated TAA-induced liver injury in WT mice, as evidenced by serum levels of ALT and AST and pathological examination (Supplementary Figs. 5D and E).

To determine the critical role of PINK1 signaling in regulating mitophagy, we overexpressed PINK1 in XBP1 HKO mice by AAV-PINK1 (Supplementary Fig. 6A). Overexpression of PINK1 increased protein levels of PINK1/Parkin and LC3-II but decreased protein levels of P62 in hepatocytes from XBP1 HKO mice (Supplementary Fig. 6B), leading to attenuated liver injury (Supplementary Figs. 6C–E).

These data suggested that mitophagy inhibition by XBP1 deficiency aggravated the mitochondrial injury and hepatocyte pyroptosis, ultimately leading to increased hepatocellular mtDNA release and enhanced macrophage STING activation during TAA-induced liver injury.

3.7. Activation of XBP1-mediated hepatocellular mitophagy and pyroptosis and macrophage STING signaling pathway in patients with ALI

To test the clinical significance of XBP1 in regulating hepatocellular mitophagy and pyroptosis and macrophage STING activation during ALI, we collected liver tissues from patients with or without ALI, and the above signaling pathways were analyzed. Significantly increased protein levels of XBP1s were observed in livers from patients with ALI (Fig. 7A). ALI induced hepatocellular mitophagy and pyroptosis as indicated by enhanced immunofluorescence staining of LC3, cleaved-caspase-1, and GSDMD-NT in ALB-positive hepatocytes (Fig. 7B). Furthermore, enhanced staining of cGAS, STING, and P-TBK1 was observed in CD68-positive macrophages as well (Fig. 7C). These data suggested the critical role of XBP1 in regulating mitophagy and pyroptosis of hepatocytes and STING signaling of macrophages during human ALI.

3.8. Hepatocyte-specific XBP1 deficiency activated macrophage STING signaling in LPS-induced acute liver injury model

In order to verify the generality of above findings of hepatocyte XBP1 in regulating macrophage STING signaling, another mouse model of liver injury induced by LPS were applied. Similarly, the protein and mRNA levels of XBP1s were increased in the livers after LPS challenge (Supplementary Figs. 7A–B). Hepatocyte XBP1 depletion aggravated LPS-induced liver injury as evidenced by higher levels of serum ALT and AST (Supplementary Fig. 7C), exacerbated architectural destruction (Supplementary Fig. 7D), and increased hepatocellular cell death (Supplementary Fig. 7E). Enhanced activation of macrophages STING (Supplementary Fig. 7F) and decreased activation of hepatocyte mitophagy signaling (Supplementary Fig. 7G) were observed in HKO mice after LPS treatment. Thus, these data suggested that XBP1 deficiency promotes hepatocyte pyroptosis by impairing mitophagy to activate mtDNA-cGAS-STING signaling of macrophages during acute liver injury with different causes.

4. Discussion

Hepatocellular cell death and macrophage innate immune activation contribute to the pathology of various liver diseases, during which XBP1 plays an important role. However, the effects of XBP1 on TAA-induced ALI and whether and how XBP1 could regulate hepatocellular pyroptosis and macrophage STING activation remains largely unknown. The principal findings of this study described the presence and mechanism of hepatocyte-specific XBP1 deficiency in regulating TAA-induced ALI. We demonstrated that XBP1 deficiency promoted mitochondrial ROS production by impairing mitophagy activation, resulting in hepatocytes pyroptosis via the NLRP3/caspase-1/GSDMD signaling pathway. Increased pyroptosis in XBP1 deficient hepatocytes facilitated the extracellular release of mtDNA, which subsequently induced macrophage STING activation in a cGAS-dependent manner (see Fig. 8).

Macrophages, the most abundant liver immune cells, play a critical role in maintaining tissue homeostasis and inflammatory liver diseases [17]. During acute liver injury and failure, DAMPs released from stressed or injured hepatocytes trigger macrophage activation, leading to inflammatory cytokine and chemokine release [18,19]. The contributory role of macrophages derived cytokines (TNF-α, IFN-γ), chemokines (MCP-1, IL-18) [20] and reactive oxygen/nitrogen species [21] results in the hepatocyte death and the recruitment of additional immune cells that booster hepatic injury [22]. Moreover, macrophages promote resolution responses by switching their functional characteristics from pro-inflammatory to anti-inflammatory in response to tissue injury [23–25]. We previously found that suppressing of proinflammatory immune activation by restraining macrophage migration protected against ischemic liver injury [26]. Infiltration of macrophages into the liver is a hallmark and cause of hepatic inflammatory injury.

The cGAS-STING signaling axis was initially found to detect pathogenic DNA triggering an innate immune response against microbial infections. Studies revealed that cGAS-STING could also be activated by endogenous DNA, which played an essential role in autoimmunity, sterile inflammatory responses, and cellular senescence [27]. Under certain cellular stresses, endogenous genomic and mitochondrial DNA

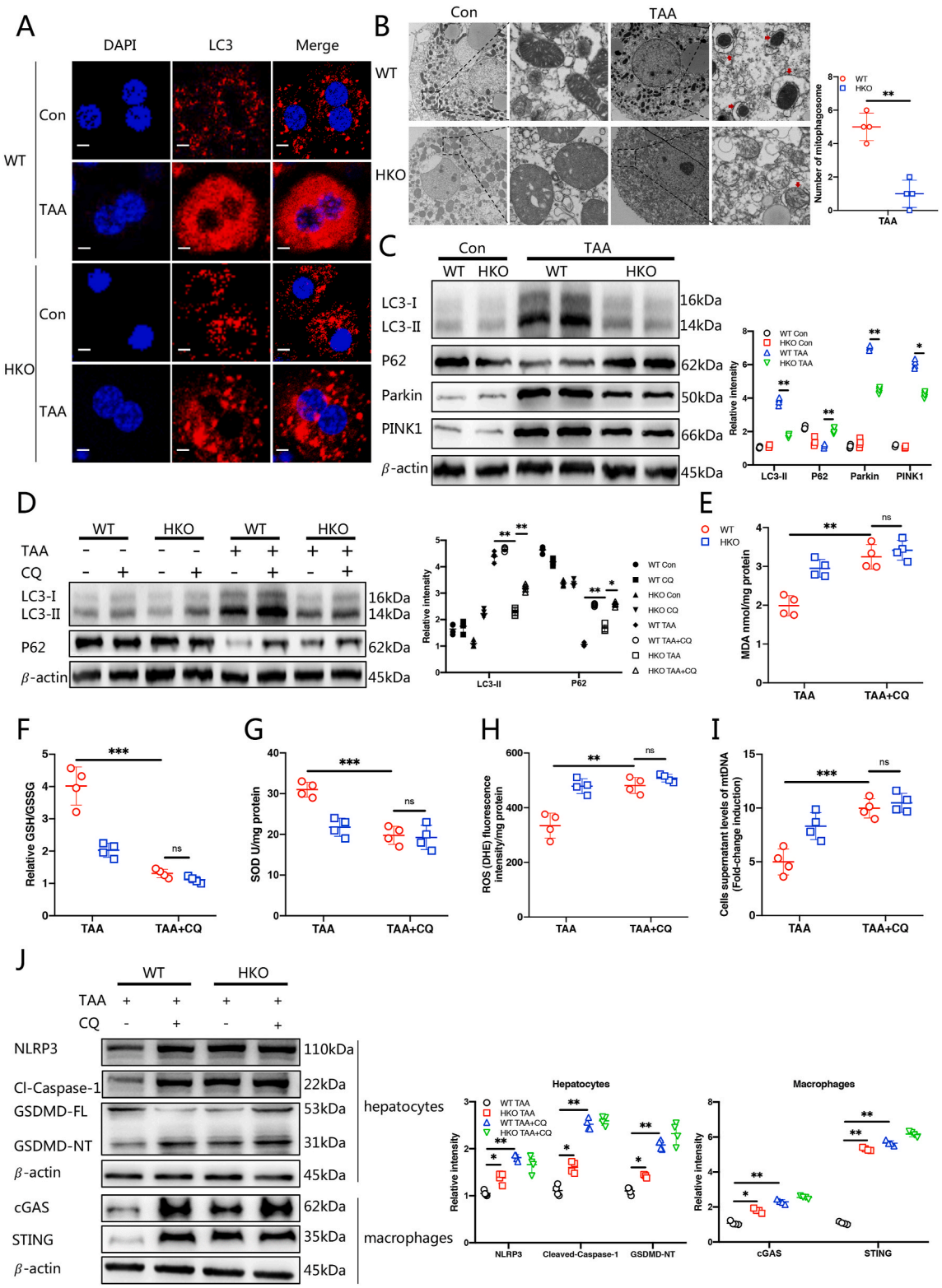

Fig. 6. Impaired mitophagy contributed to ROS-mediated pyroptosis of XBP1 deficient hepatocytes and subsequent macrophage STING activation during TAA-induced acute liver injury.

(A and B) Primary hepatocytes isolated from the liver of WT and HKO mice were stimulated with TAA. Staining with LC3 (red) and DAPI (blue). Scale bar, 100 μm (A). Mitophagic microstructures seen using transmission electron microscopy. Scale bars, 1.6 and 0.33 μm (B). (C) Hepatocytes were isolated from livers post-TAA treatment to analyze the expression of P62, LC3-I, LC3-II, Parkin, Pink1, and β-actin using western blotting. (D) Primary hepatocytes were pre-treated with or without CQ before TAA stimulation. Representative Western blot images of P62, LC3-I, LC3-II and β-actin. (E–H) MDA, GSH/GSSG, and ROS levels and SOD activity in liver tissues. (I) Levels of mtDNA in the supernatant of primary hepatocytes post-TAA stimulation with or without CQ pre-treatment. (J) Hepatocytes and intrahepatic macrophages were isolated from livers post-TAA treatment with or without CQ pre-treatment to analyze the expression of NLRP3, cleaved caspase-1, GSDMD-NT, GSDMD-FL, cGAS, STING, and β-actin using western blotting. Data are presented as the mean ± SEM (n = 4). *P < 0.05, **P < 0.01, ***P < 0.001. NS, not significant. (For interpretation of the references to colour in this figure legend, the reader is referred to the Web version of this article.)

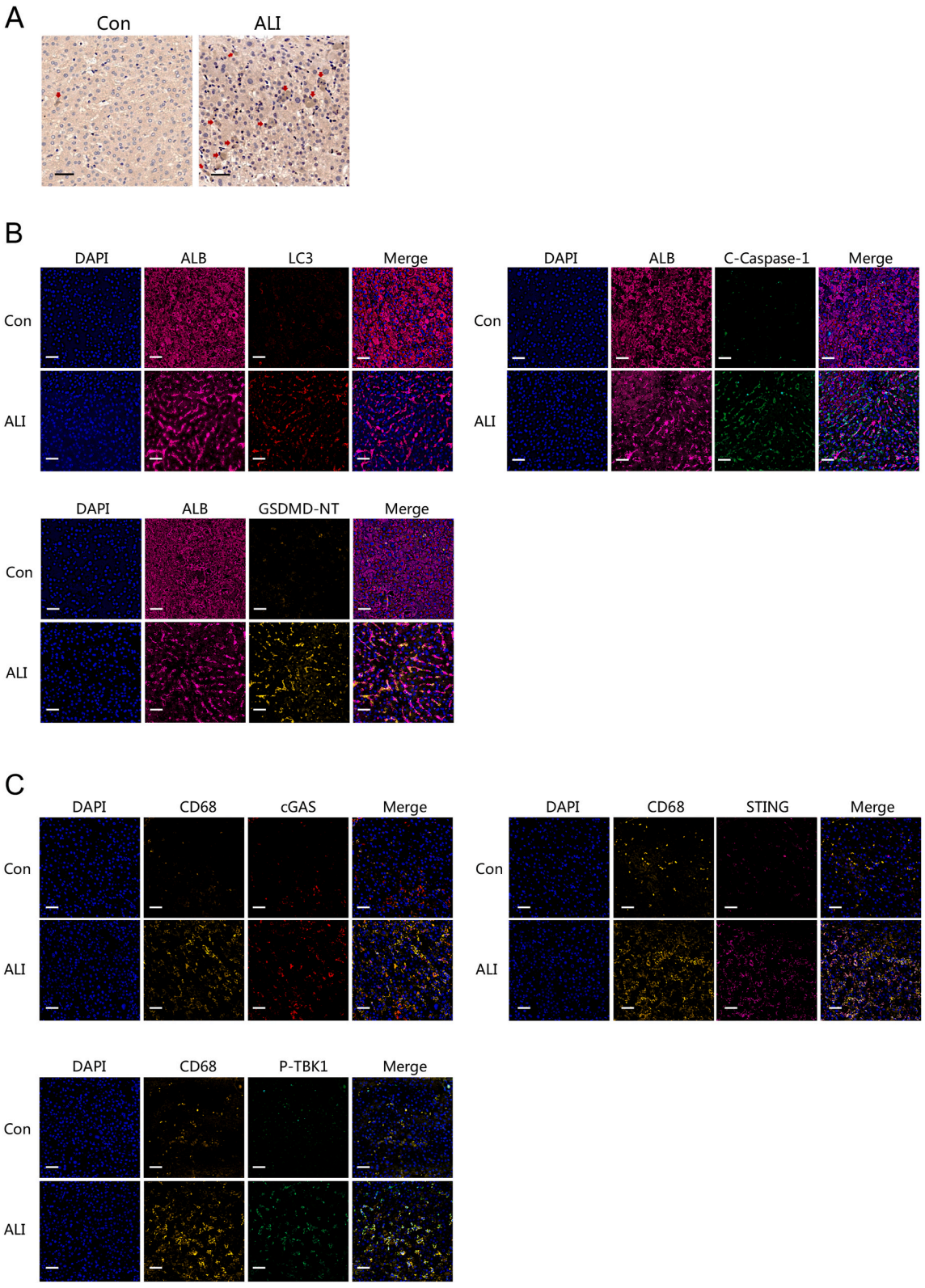

Fig. 7. Activation of XBP1-mediated hepatocellular mitophagy and pyroptosis and macrophage STING signaling pathway in patients with ALI.
Human liver tissues were collected from five patients with ALI and five controls. (A) IHC XBP1s-stained liver tissue sections. Scale bar, 50 μm. Immunofluorescence staining of liver tissue sections from each group. Albumin (pink), LC3 (red), cleaved caspase-1 (green), GSDMD-NT (yellow), and DAPI (blue). Scale bar, 50 μm (B) and CD68 (yellow), cGAS (red), STING (pink), P-TBK1 (green) and DAPI (blue). Scale bar, 50 μm (C). Data are presented as the mean ± SEM (n = 5). *P < 0.05, **P < 0.01, ***P < 0.001. NS, not significant; IHC, immunohistochemistry. (For interpretation of the references to colour in this figure legend, the reader is referred to the Web version of this article.)

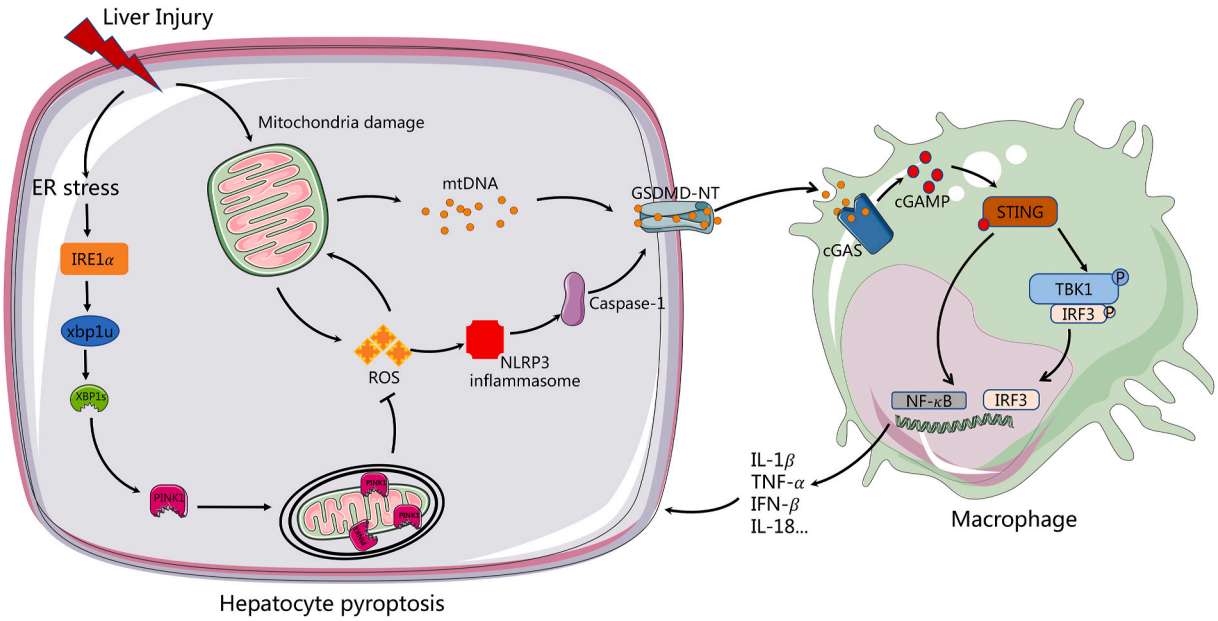

Fig. 8. Scheme showing that XBP1 deficiency promotes hepatocyte pyroptosis by impairing mitophagy to activate mtDNA/cGAS/STING signalling of macrophages.

can enter the cytoplasm to further activate cGAS and subsequent immune and inflammatory responses [28]. Growing evidence suggests that macrophage STING activation is an important driver of various liver diseases. Increased STING activation in macrophages was found in human and murine livers with non-alcoholic steatohepatitis [29,30]. Experimental CCl4-induced liver fibrosis and enhanced cGAS/STING activation in liver tissues [31], whereas STING deficiency attenuated liver inflammation and fibrosis [32]. In an earlier study, we demonstrated that mtDNA release from injured hepatocytes promoted macrophage STING activation in the context of acute ischemic liver injury in aged mice [16]. Although mtDNA with or without TAA pre-treatment showed no significant difference in the activation of STING signaling, whether or not the mtDNA could be modified by TAA treatment is still unclear. Indeed, oxidized mtDNA generated under oxidative stress reportedly activated NLRP3 inflammasome activation and inflammation [33]. The evidence of oxidized mtDNA in regulating STING signaling is still lacking and warrants further study.

Pyroptosis is morphologically and mechanistically distinct from other forms of cell death, which was initially defined as caspase-1-dependent necrotic death. Pyroptosis is characterised by rapid plasma membrane rupture and the release of proinflammatory intracellular contents. Following cleavage, the N-terminal domain of GSDMD targets and enters cellular membranes to form large oligomeric membrane pores, disrupting ion homeostasis and ultimately causing cell death [34]. Studies have indicated the critical role of pyroptosis in regulating many inflammatory disorders. Increased hepatocyte pyroptosis contributes to the pathology of acute and chronic liver diseases [35,36]. Hepatocyte pyroptosis mediated by GSDMD activation results in polymorphonuclear leukocyte inflammation and alcoholic hepatitis [37]. NLRP3 inflammasome activation contributes to hepatocyte pyroptosis, liver inflammation, and fibrosis in mice [38]. Furthermore, caspase-1- and GSDMD-mediated pyroptosis of hepatocytes propagated liver fibrosis development by releasing inflammasome components to induce stellate cell activation [39]. We observed that pyroptosis facilitated the extracellular release of mtDNA and subsequent macrophage STING activation. Consistently, GSDMD was found to be able to trigger a rapid mitochondrial collapse along with the initial cytosolic accumulation of mtDNA, promoting mtDNA release from the cell when the plasma membrane ruptured [40].

ROS are abundantly produced in TAA-treated livers and play an important role in the pathogenesis of TAA-induced liver injury. Strategies targeting ROS scavenging play a protective role in TAA-induced liver injury [41,42]. The critical role of ROS in mediating pyroptosis has also been reported. Iron activates ROS signaling to induce pyroptosis in melanoma cells [43]. Furthermore, ROS promote pore formation downstream of GSDMD cleavage [44]. Upregulation of ROS levels exerts antitumor effects by triggering pyroptosis [45]. Increased ROS-NLRP3-caspase-1-GSDMD activation and pyroptosis were observed in hepatocytes after TAA-induced liver injury. Moreover, ROS has been suggested as a crucial element for NLRP3 activation [46]. ROS-mediated NLRP3 activation contributes to the antibacterial host defense by macrophages [47]. However, ROS-independent NLRP3 inflammasome activation has recently been identified. Mitochondrial cardiolipin activates the NLRP3 inflammasome through the direct binding of NLRP3 to cardiolipin [48].

Mitochondria play a key role in various cellular processes including ROS generation, cell death, and survival [4]. Mitophagy is a conserved cellular adaptive response that selectively eliminates dysfunctional mitochondria by targeting them to the autophagosome for degradation. Defective mitophagy contributes to both alcoholic liver [49] and non-alcoholic fatty liver diseases [50]. Because mitochondria are a primary source of ROS, mitophagy is essential for ROS clearance [51]. Impaired mitophagy may result in the accumulation of damaged mitochondria and the dysregulation of free radical scavenging. In the present study, increased ROS expression, cytosolic mtDNA accumulation, and extracellular release, but impaired mitophagy, were observed in TAA-treated hepatocytes. Mitochondrial ROS scavenging decreased NLRP3 activation and attenuated hepatocyte pyroptosis. These findings suggest that overexpression of mitochondrial ROS, owing to impaired mitophagy promotes hepatocyte pyroptosis. Consistently, hepatocyte-specific FUNDC1 ablation inhibits mitophagy and the accumulation of dysfunctional mitochondria and triggers cytosolic mtDNA release and caspase-1 activation [52]. Mitophagy-related cell death has also been reported. Mitophagy was triggered by ketoconazole-induced hepatocellular carcinoma cell apoptosis [53]. It has been found that the PINK1 expression was increased post mitophagy activation. Moreover, while PINK1 knockdown efficiently inhibited mitophagy activation, PINK1 overexpression activated mitophagy [54,55]. These findings suggested that the intracellular levels of PINK1 expression play an important role in activating mitophagy. In the present study, we also observed XBP1 inhibition downregulated the expression of PINK1 and suppressed mitophagy activation. However,

many studies have established the critical role of PINK1-mediated mitochondrial ubiquitination during mitophagy activation [56]. Therefore, increased PINK1 expression by XBP1 activation may activating mitophagy activation by promoting PINK1-mediated mitochondrial ubiquitination, which remains to be further studied.

ER stress initiates cell death and inflammatory mechanisms; C/EBP homologous protein activation induces NLRP3 inflammasome activation and hepatocyte pyroptosis [57]. Inhibition of IRE-1a/XBP-1 significantly attenuated NLRP3 inflammasome activation and pyroptosis in human renal tubular epithelial cells. Emerging evidence has also suggested an interplay between ER stress, autophagy, and mitophagy [58]. All three branches of the UPR can regulate autophagy, although the precise regulation of induction or inhibition is cell- and context-specific [59]. Paneth cell-specific deletion of XBP1 results in ER stress, autophagy induction, and spontaneous ileitis [60]. Unspliced XBP1 suppressed autophagy by promoting the degradation of FoxO1 in cancer cells [61]. Contrastingly, oxidative stress-induced UPR based on the splicing of XBP1 mRNA triggered autophagy in hepatic stellate cells [8]. Recent studies have revealed the critical role of XBP1s in various liver diseases. XBP1s was able to bind to the hepatic 12-h cistrome, and hepatocyte XBP1 ablation disrupted the 12-h clock to promote NAFLD development [62]. Another study also found increased liver injury, apoptosis, and fibrosis in hepatocyte XBP1 deficient mice [63]. Although ER stress and autophagy can function independently, they share some features including cytoprotection by alleviating stress. Liver-specific XBP1 knockout mice showed impaired UPS and increased susceptibility to bile acid-induced liver injury [64]. A study also found that hepatocyte-specific XBP1 depletion sensitised mice to liver injury through IRE1a hyperactivation [65]. However, the induction of cell death under conditions of extreme or unresolved ER stress has also been reported [66]. IRE1a activation promotes mitochondrial ROS production and NLRP3- and caspase-2-driven mitochondrial damage [67]. Similarly, another study showed that IRE1a activated the NLRP3 inflammasome and promoted programmed cell death under irremediable ER stress [68].

5. Conclusions

In conclusion, we have identified a novel role for XBP1 in regulating hepatocyte pyroptosis and STING signaling activation in macrophages during ALI. We elucidated that XBP1 deficiency promotes ROS/NLRP3/caspase-1/GSDMD-mediated pyroptosis in hepatocytes by inhibiting mitophagy, which facilitates the extracellular release of mtDNA to further activate macrophage inflammatory response via the cGAS-STING signaling pathway. Our study suggests that strategies targeting hepatocyte pyroptosis, macrophage STING activation and XBP1 signaling may provide a promising approach to ameliorate human ALI.

Author contribution

Authors' contributions: Zheng Liu, Mingming Wang, Xun Wang, Qingfa Bu, Qi Wang, Wantong Su, Lei Li: performed the experiments and analyzed the data. Haoming Zhou, Ling Lu: designed the experiments and drafted the manuscript.

Declaration of competing interest

The authors declare that they have no conflict of interest.

Acknowledgements

Founding. This study was supported by grants from the National Natural Science Foundation of China (81971495, 91442117, 82071798), the CAMS Innovation Fund for Medical Sciences (No. 2019-I2M-5–035), the National Science Foundation of Jiangsu Province (BRA2017533, BK20191490), the State Key Laboratory of Reproductive Medicine (SKLRM-K202001) and the Foundation of Jiangsu Collaborative Innovation Center of Biomedical Functional Materials. The sponsors had no role in study design; in the collection, analysis, and interpretation of data; in the writing of the report; and in the decision to submit the article for publication.

Appendix A. Supplementary data

Supplementary data to this article can be found online at https://doi.org/10.1016/j.redox.2022.102305.

References

[1] P. Yu, X. Zhang, N. Liu, L. Tang, C. Peng, X. Chen, Pyroptosis: mechanisms and diseases, Signal Transduct Target Ther 6 (1) (2021) 128.
[2] X. Wang, X. Li, S. Liu, A.N. Brickell, J. Zhang, Z. Wu, et al., PCSK9 regulates pyroptosis via mtDNA damage in chronic myocardial ischemia, Basic Res. Cardiol. 115 (6) (2020) 66.
[3] C. Brenner, L. Galluzzi, O. Kepp, G. Kroemer, Decoding cell death signals in liver inflammation, J. Hepatol. 59 (3) (2013) 583–594.
[4] K. Palikaras, E. Lionaki, N. Tavernarakis, Mechanisms of mitophagy in cellular homeostasis, physiology and pathology, Nat. Cell Biol. 20 (9) (2018) 1013–1022.
[5] J. Yu, H. Nagasu, T. Murakami, H. Hoang, L. Broderick, H.M. Hoffman, et al., Inflammasome activation leads to Caspase-1-dependent mitochondrial damage and block of mitophagy, Proc. Natl. Acad. Sci. U. S. A. 111 (43) (2014) 15514–15519.
[6] H.H. Pua, J. Guo, M. Komatsu, Y.W. He, Autophagy is essential for mitochondrial clearance in mature T lymphocytes, J. Immunol. 182 (7) (2009) 4046–4055.
[7] L.A. Sena, N.S. Chandel, Physiological roles of mitochondrial reactive oxygen species, Mol. Cell. 48 (2) (2012) 158–167.
[8] V. Hernandez-Gea, M. Hilscher, R. Rozenfeld, M.P. Lim, N. Nieto, S. Werner, et al., Endoplasmic reticulum stress induces fibrogenic activity in hepatic stellate cells through autophagy, J. Hepatol. 59 (1) (2013) 98–104.
[9] C. Hetz, K. Zhang, R.J. Kaufman, Mechanisms, regulation and functions of the unfolded protein response, Nat. Rev. Mol. Cell Biol. 21 (8) (2020) 421–438.
[10] J.R. Cubillos-Ruiz, S.E. Bettigole, L.H. Glimcher, Tumorigenic and immunosuppressive effects of endoplasmic reticulum stress in cancer, Cell 168 (4) (2017) 692–706.
[11] X. Le, J. Mu, W. Peng, J. Tang, Q. Xiang, S. Tian, et al., DNA methylation downregulated ZDHHC1 suppresses tumor growth by altering cellular metabolism and inducing oxidative/ER stress-mediated apoptosis and pyroptosis, Theranostics 10 (21) (2020) 9495–9511.
[12] J. Huang, W. Lu, D.M. Doycheva, M. Gamdzyk, X. Hu, R. Liu, et al., IRE1alpha inhibition attenuates neuronal pyroptosis via miR-125/NLRP1 pathway in a neonatal hypoxic-ischemic encephalopathy rat model, J. Neuroinflammation 17 (1) (2020) 152.
[13] X. Chou, F. Ding, X. Zhang, X. Ding, H. Gao, Q. Wu, Sirtuin-1 ameliorates cadmium-induced endoplasmic reticulum stress and pyroptosis through XBP-1s deacetylation in human renal tubular epithelial cells, Arch. Toxicol. 93 (4) (2019) 965–986.
[14] D. Xu, Y. Tian, Q. Xia, B. Ke, The cGAS-STING pathway: novel perspectives in liver diseases, Front. Immunol. 12 (2021) 682736.
[15] H. Zhou, H. Wang, M. Ni, S. Yue, Y. Xia, R.W. Busuttil, et al., Glycogen synthase kinase 3beta promotes liver innate immune activation by restraining AMP-activated protein kinase activation, J. Hepatol. 69 (1) (2018) 99–109.
[16] W. Zhong, Z. Rao, J. Rao, G. Han, P. Wang, T. Jiang, et al., Aging aggravated liver ischemia and reperfusion injury by promoting STING-mediated NLRP3 activation in macrophages, Aging Cell 19 (8) (2020), e13186.
[17] O. Krenkel, F. Tacke, Liver macrophages in tissue homeostasis and disease, Nat. Rev. Immunol. 17 (5) (2017) 306–321.
[18] W. Bernal, J. Wendon, Acute liver failure, N. Engl. J. Med. 369 (26) (2013) 2525–2534.
[19] F. Tacke, Targeting hepatic macrophages to treat liver diseases, J. Hepatol. 66 (6) (2017) 1300–1312.
[20] C.G. Antoniades, P.A. Berry, J.A. Wendon, D. Vergani, The importance of immune dysfunction in determining outcome in acute liver failure, J. Hepatol. 49 (5) (2008) 845–861.
[21] S.L. Michael, N.R. Pumford, P.R. Mayeux, M.R. Niesman, J.A. Hinson, Pretreatment of mice with macrophage inactivators decreases acetaminophen hepatotoxicity and the formation of reactive oxygen and nitrogen species, Hepatology 30 (1) (1999) 186–195.
[22] T. Luedde, R.F. Schwabe, NF-kappaB in the liver–linking injury, fibrosis and hepatocellular carcinoma, Nat. Rev. Gastroenterol. Hepatol. 8 (2) (2011) 108–118.
[23] L. Arnold, A. Henry, F. Poron, Y. Baba-Amer, N. van Rooijen, A. Plonquet, et al., Inflammatory monocytes recruited after skeletal muscle injury switch into antiinflammatory macrophages to support myogenesis, J. Exp. Med. 204 (5) (2007) 1057–1069.
[24] M. Nahrendorf, F.K. Swirski, E. Aikawa, L. Stangenberg, T. Wurdinger, J. L. Figueiredo, et al., The healing myocardium sequentially mobilizes two monocyte subsets with divergent and complementary functions, J. Exp. Med. 204 (12) (2007) 3037–3047.
[25] M.H. Sieweke, J.E. Allen, Beyond stem cells: self-renewal of differentiated macrophages, Science 342 (6161) (2013) 1242974.

[26] H. Zhou, S. Zhou, Y. Shi, Q. Wang, S. Wei, P. Wang, et al., TGR5/Cathepsin E signaling regulates macrophage innate immune activation in liver ischemia and reperfusion injury, Am. J. Transplant. 21 (4) (2021) 1453–1464.
[27] K.P. Hopfner, V. Hornung, Molecular mechanisms and cellular functions of cGAS-STING signalling, Nat. Rev. Mol. Cell Biol. 21 (9) (2020) 501–521.
[28] X. Zhang, X.C. Bai, Z.J. Chen, Structures and mechanisms in the cGAS-STING innate immunity pathway, Immunity 53 (1) (2020) 43–53.
[29] Y. Yu, Y. Liu, W. An, J. Song, Y. Zhang, X. Zhao, STING-mediated inflammation in Kupffer cells contributes to progression of nonalcoholic steatohepatitis, J. Clin. Invest. 129 (2) (2019) 546–555.
[30] X. Luo, H. Li, L. Ma, J. Zhou, X. Guo, S.L. Woo, et al., Expression of STING is increased in liver tissues from patients with NAFLD and promotes macrophage-mediated hepatic inflammation and fibrosis in mice, Gastroenterology 155 (6) (2018) 1971–19784 e4.
[31] H. Yong, S. Wang, F. Song, Activation of cGAS/STING pathway upon TDP-43-mediated mitochondrial injury may be involved in the pathogenesis of liver fibrosis, Liver Int. 41 (8) (2021) 1969–1971.
[32] A. Iracheta-Vellve, J. Petrasek, B. Gyongyosi, A. Satishchandran, P. Lowe, K. Kodys, et al., Endoplasmic reticulum stress-induced hepatocellular death pathways mediate liver injury and fibrosis via stimulator of interferon genes, J. Biol. Chem. 291 (52) (2016) 26794–26805.
[33] H. Xian, Y. Liu, A. Rundberg Nilsson, R. Gatchalian, T.R. Crother, W. G. Tourtellotte, et al., Metformin inhibition of mitochondrial ATP and DNA synthesis abrogates NLRP3 inflammasome activation and pulmonary inflammation, Immunity 54 (7) (2021) 1463–1477 e11.
[34] P. Broz, P. Pelegrin, F. Shao, The gasdermins, a protein family executing cell death and inflammation, Nat. Rev. Immunol. 20 (3) (2020) 143–157.
[35] J. Gautheron, G.J. Gores, C.M.P. Rodrigues, Lytic cell death in metabolic liver disease, J. Hepatol. 73 (2) (2020) 394–408.
[36] J. Wu, S. Lin, B. Wan, B. Velani, Y. Zhu, Pyroptosis in liver disease: new insights into disease mechanisms, Aging Dis 10 (5) (2019) 1094–1108.
[37] E. Khanova, R. Wu, W. Wang, R. Yan, Y. Chen, S.W. French, et al., Pyroptosis by caspase11/4-gasdermin-D pathway in alcoholic hepatitis in mice and patients, Hepatology 67 (5) (2018) 1737–1753.
[38] A. Wree, A. Eguchi, M.D. McGeough, C.A. Pena, C.D. Johnson, A. Canbay, et al., NLRP3 inflammasome activation results in hepatocyte pyroptosis, liver inflammation, and fibrosis in mice, Hepatology 59 (3) (2014) 898–910.
[39] S. Gaul, A. Leszczynska, F. Alegre, B. Kaufmann, C.D. Johnson, L.A. Adams, et al., Hepatocyte pyroptosis and release of inflammasome particles induce stellate cell activation and liver fibrosis, J. Hepatol. 74 (1) (2021) 156–167.
[40] C. de Torre-Minguela, A.I. Gomez, I. Couillin, P. Pelegrin, Gasdermins mediate cellular release of mitochondrial DNA during pyroptosis and apoptosis, Faseb. J. 35 (8) (2021), e21757.
[41] H.Y. Li, Y. Chien, Y.J. Chen, S.F. Chen, Y.L. Chang, C.H. Chiang, et al., Reprogramming induced pluripotent stem cells in the absence of c-Myc for differentiation into hepatocyte-like cells, Biomaterials 32 (26) (2011) 5994–6005.
[42] N.Q. Dat, L.T.T. Thuy, V.N. Hieu, H. Hai, D.V. Hoang, N. Thi Thanh Hai, et al., Hexa histidine-tagged recombinant human cytoglobin deactivates hepatic stellate cells and inhibits liver fibrosis by scavenging reactive oxygen species, Hepatology 73 (6) (2021) 2527–2545.
[43] B. Zhou, J.Y. Zhang, X.S. Liu, H.Z. Chen, Y.L. Ai, K. Cheng, et al., Tom20 senses iron-activated ROS signaling to promote melanoma cell pyroptosis, Cell Res. 28 (12) (2018) 1171–1185.
[44] C.L. Evavold, I. Hafner-Bratkovic, P. Devant, J.M. D'Andrea, E.M. Ngwa, E. Borsic, et al., Control of gasdermin D oligomerization and pyroptosis by the Ragulator-Rag-mTORC1 pathway, Cell 184 (17) (2021) 4495–4511, e19.
[45] D. Jia, L. Gong, Y. Li, S. Cao, W. Zhao, L. Hao, et al., {BiW8 O30 } exerts antitumor effect by triggering pyroptosis and upregulating reactive oxygen species, Angew Chem. Int. Ed. Engl. 60 (39) (2021) 21449–21456.
[46] J. Tschopp, K. Schroder, NLRP3 inflammasome activation: the convergence of multiple signalling pathways on ROS production? Nat. Rev. Immunol. 10 (3) (2010) 210–215.
[47] J. Garaude, R. Acin-Perez, S. Martinez-Cano, M. Enamorado, M. Ugolini, E. Nistal-Villan, et al., Mitochondrial respiratory-chain adaptations in macrophages contribute to antibacterial host defense, Nat. Immunol. 17 (9) (2016) 1037–1045.
[48] S.S. Iyer, Q. He, J.R. Janczy, E.I. Elliott, Z. Zhong, A.K. Olivier, et al., Mitochondrial cardiolipin is required for Nlrp3 inflammasome activation, Immunity 39 (2) (2013) 311–323.
[49] H. Zhou, P. Zhu, J. Wang, S. Toan, J. Ren, DNA-PKcs promotes alcohol-related liver disease by activating Drp1-related mitochondrial fission and repressing FUNDC1-required mitophagy, Signal Transduct Target Ther 4 (2019) 56.
[50] L. Wang, X. Liu, J. Nie, J. Zhang, S.R. Kimball, H. Zhang, et al., ALCAT1 controls mitochondrial etiology of fatty liver diseases, linking defective mitophagy to steatosis, Hepatology 61 (2) (2015) 486–496.
[51] R. Scherz-Shouval, Z. Elazar, Regulation of autophagy by ROS: physiology and pathology, Trends Biochem. Sci. 36 (1) (2011) 30–38.
[52] W. Li, Y. Li, S. Siraj, H. Jin, Y. Fan, X. Yang, et al., FUN14 domain-containing 1-mediated mitophagy suppresses hepatocarcinogenesis by inhibition of inflammasome activation in mice, Hepatology 69 (2) (2019) 604–621.
[53] Y. Chen, H.N. Chen, K. Wang, L. Zhang, Z. Huang, J. Liu, et al., Ketoconazole exacerbates mitophagy to induce apoptosis by downregulating cyclooxygenase-2 in hepatocellular carcinoma, J. Hepatol. 70 (1) (2019) 66–77.
[54] W.N. Kong, W. Li, C. Bai, Y. Dong, Y. Wu, W. An, Augmenter of liver regeneration-mediated mitophagy protects against hepatic ischemia/reperfusion injury, Am. J. Transplant. 22 (1) (2022) 130–143.
[55] Y. Xu, J. Lu, Y. Tang, W. Xie, H. Zhang, B. Wang, et al., PINK1 deficiency in gastric cancer compromises mitophagy, promotes the Warburg effect, and facilitates M2 polarization of macrophages, Cancer Lett. 529 (2022) 19–36.
[56] A. Eiyama, K. Okamoto, PINK1/Parkin-mediated mitophagy in mammalian cells, Curr. Opin. Cell Biol. 33 (2015) 95–101.
[57] C. Lebeaupin, E. Proics, C.H. de Bieville, D. Rousseau, S. Bonnafous, S. Patouraux, et al., ER stress induces NLRP3 inflammasome activation and hepatocyte death, Cell Death Dis. 6 (2015), e1879.
[58] A.V. Cybulsky, Endoplasmic reticulum stress, the unfolded protein response and autophagy in kidney diseases, Nat. Rev. Nephrol. 13 (11) (2017) 681–696.
[59] H.O. Rashid, R.K. Yadav, H.R. Kim, H.J. Chae, ER stress: autophagy induction, inhibition and selection, Autophagy 11 (11) (2015) 1956–1977.
[60] T.E. Adolph, M.F. Tomczak, L. Niederreiter, H.J. Ko, J. Bock, E. Martinez-Naves, et al., Paneth cells as a site of origin for intestinal inflammation, Nature 503 (7475) (2013) 272–276.
[61] Y. Zhao, X. Li, M.Y. Cai, K. Ma, J. Yang, J. Zhou, et al., XBP-1u suppresses autophagy by promoting the degradation of FoxO1 in cancer cells, Cell Res. 23 (4) (2013) 491–507.
[62] H. Meng, N.M. Gonzales, D.M. Lonard, N. Putluri, B. Zhu, C.C. Dacso, et al., XBP1 links the 12-hour clock to NAFLD and regulation of membrane fluidity and lipid homeostasis, Nat. Commun. 11 (1) (2020) 6215.
[63] S. Olivares, A.S. Henkel, Hepatic Xbp1 gene deletion promotes endoplasmic reticulum stress-induced liver injury and apoptosis, J. Biol. Chem. 290 (50) (2015) 30142–30151.
[64] A. Kriegermeier, A. Hyon, M. Sommars, S. Hubchak, B. LeCuyer, X. Liu, et al., Hepatic X-box binding protein 1 and unfolded protein response is impaired in weanling mice with resultant hepatic injury, Hepatology 74 (6) (2021) 3362–3375.
[65] C.C. Duwaerts, K. Siao, R.K. Soon Jr., C. Her, T. Iwawaki, K. Kohno, et al., Hepatocyte-specific deletion of XBP1 sensitizes mice to liver injury through hyperactivation of IRE1alpha, Cell Death Differ. 28 (5) (2021) 1455–1465.
[66] C. Lebeaupin, D. Vallee, Y. Hazari, C. Hetz, E. Chevet, B. Bailly-Maitre, Endoplasmic reticulum stress signalling and the pathogenesis of non-alcoholic fatty liver disease, J. Hepatol. 69 (4) (2018) 927–947.
[67] D.N. Bronner, B.H. Abuaita, X. Chen, K.A. Fitzgerald, G. Nunez, Y. He, et al., Endoplasmic reticulum stress activates the inflammasome via NLRP3- and caspase-2-driven mitochondrial damage, Immunity 43 (3) (2015) 451–462.
[68] A.G. Lerner, J.P. Upton, P.V. Praveen, R. Ghosh, Y. Nakagawa, A. Igbaria, et al., IRE1alpha induces thioredoxin-interacting protein to activate the NLRP3 inflammasome and promote programmed cell death under irremediable ER stress, Cell Metabol. 16 (2) (2012) 250–264.